

A Systematic Approach to Noncoherent Detection for DPSK Modulation in Multiuser Correlated Diversity Rayleigh Fading Channels

Mahesh K. Varanasi and Matthias Brehler

Abstract — A correlated diversity Rayleigh fading (CDRF) channel models inter-diversity fading and signal correlations. This paper considers the multiuser CDRF channel wherein several users transmit information simultaneously using signals with inter-diversity as well as inter-user correlations. Each user employs DPSK modulation. Besides allowing simple noncoherent detection without channel estimation algorithms, DPSK is a modulation method of choice when the coherence time of the channel is too short to estimate the fading coefficients accurately. Until recently, the multiuser detectors suggested for the multiuser CDRF channel have been of the post-decorrelative type with ad-hoc equal-gain combining.

A systematic approach to optimum DPSK detection for the single-user CDRF channel was introduced in [Var97]. This paper generalizes that work to the multiuser CDRF channel. As in [Var97], two different noncoherent detectors are obtained. For the slowly fading channel, where the fading coefficients are essentially constant over two successive symbol intervals, the generalized likelihood ratio test (GLRT) is derived. This rule can be implemented without knowledge of the fading statistics or the users' energies. For both slow and fast fading channels, where in the latter, the fading coefficients can vary from one symbol-interval to the next, a multiuser minimum error probability (MEP) detector is also obtained. The MEP requires a limited knowledge of the statistics of the fading coefficients for its implementation. Upper and lower bounds on the bit error rate (BER) of the MEP and GLRT detectors are derived. In our numerical examples, these bounds converge for high signal-to-noise ratios for each detector. While these detectors are exponentially complex, their performances provide benchmarks for sub-optimal detectors. In particular, it is seen that the post-decorrelative detectors can be far from satisfactory.

I. INTRODUCTION

The fading processes associated with multiple diversity branches are often assumed to be mutually independent and sometimes to even have equal signal strengths (hence independent and identically distributed). While such assumptions avoid the analytical difficulties of dealing with correlated diversity channels, they can often be too restrictive to model realistic systems. For example, in receiver antenna diversity

systems, the fading processes of the diversity branches will be highly correlated if the antennas cannot be separated sufficiently (cf. [Jak93]). Space restrictions can indeed be severe in many applications, as on hand-held communication devices. We refer to the correlation between the fading processes across diversity branches as *inter-diversity fading correlation*. Such correlation may also result in frequency or time diversity systems due to restrictions in either of those resources [Jak93]. *Inter-diversity signal correlation* arises for instance in multipath systems, where the signal bandwidth is sufficiently large to resolve multiple fading paths but is still limited enough so that the time translates of a user's signal are correlated. Inter-diversity signal correlation leads to correlation in additive noise after matched filtering the received signal. Hence, the CDRF model applies when resources (space, time, bandwidth) are limited as in systems that employ *diversity with discipline*. In addition to the inter-diversity correlations for each user, there are *inter-user signal correlations* (which translate to further noise correlation) in bandwidth-efficient multi-user systems.

Coherent detection in fading channels is premised on the availability of perfect knowledge of the fading parameters (cf. [Var96] or [ZB96]). In practice, these parameters must be estimated. The quality of the estimates depends on how slowly or rapidly the channel fades, and in decision-directed estimators, the phase-reversal phenomenon due to the effect of error propagation can be the limiting factor [WDH94]. A nice feature of DPSK modulation is that it avoids the expense of elaborate channel estimation algorithms as well as the vulnerability to the phase reversal phenomenon [Var97].

In DPSK the information is encoded in the phase difference between two successive symbol transmissions, so that it is usually required that the fading coefficients stay constant over two successive symbol intervals. Channels where such an assumption is valid will be referred to as *slowly fading* channels in this paper. However, *fast fading* channels are also considered where we define fast fading to mean that the fading parameters are allowed to vary from one symbol interval to the next (but not within a symbol interval). The slow fading assumption holds for lower vehicular speeds and/or higher data rates and/or higher carrier frequencies when compared to the fast fading channel.

In [Var97], a systematic framework was introduced for noncoherent detection for DPSK modulation in the single-user CDRF channel. The inter-diversity fading and signal correlations were fully accounted for in the specification of the MEP detector, while the GLRT detector was obtained for slowly fading channels for applications where the knowledge of fading correlations is not acquired. The MEP and the GLRT detectors were used to specify the post-decorrelative

Mahesh K. Varanasi is with the Department of Electrical and Computer Engineering at the University of Colorado in Boulder, CO 80309. Matthias Brehler is a graduate student from the Technische Universität München, Germany, currently working at the University of Colorado at Boulder. This work was supported in part by NSF Grant NCR-9725778.

combiners in a multiuser channel and the resulting detectors were seen to significantly outperform the previously proposed post-decorrelative ad-hoc equal gain combiner (cf. [Zvo94], [ZB96], and [HS94]). In this paper, we adopt a multiuser approach by generalizing the systematic approach of [Var97] to the multiuser CDRF channel.

The rest of the paper is organized as follows: after presenting the discrete-time channel model in Section II, the GLRT detector is derived in Section III and the MEP detector in Section IV. The error probability analysis is performed in Section V, where bounds on the BER of both detectors are obtained. Numerical examples are given in Section VI and conclusions are drawn in Section VII.

II. DISCRETE-TIME MODEL FOR THE MULTIUSER CORRELATED DIVERSITY RAYLEIGH FADING CHANNEL

In this section we present the discrete-time model for the K user CDRF channel with L diversity branches per user. Our model is a direct extension of the single-user model in [Var97]; specifics on how it arises from the continuous-time model are given in [Var96]. That model was described for frequency-selective multipath diversity with L resolvable paths. Other diversity techniques will also yield the same discrete-time model. The KL -dimensional vectors of observations for the zeroth and the previous symbol interval can be written as

$$\begin{aligned} \mathbf{q}(-1) &= \sqrt{\bar{\gamma}} \mathbf{R} \text{diag}\{\mathbf{r}, L\}^{1/2} \text{diag}\{\mathbf{d}(-1), L\} \mathbf{c}(-1) + \mathbf{n}(-1), \\ \mathbf{q}(0) &= \sqrt{\bar{\gamma}} \mathbf{R} \text{diag}\{\mathbf{r}, L\}^{1/2} \text{diag}\{\mathbf{d}(0), L\} \mathbf{c}(0) + \mathbf{n}(0), \end{aligned} \quad (1)$$

where $\bar{\gamma}$ is the average signal to noise ratio (SNR) of user one and \mathbf{r} is a vector containing the K users' average energy ratios relative to user one. The operator $\text{diag}\{\mathbf{x}, L\}$ repeats the elements of any vector \mathbf{x} L times and places them on the diagonal of a matrix, e.g., $\text{diag}\{[x_1, x_2]^T, 2\} = \text{diag}\{[x_1, x_1, x_2, x_2]^T\}$. $\mathbf{d}(0)$ and $\mathbf{d}(-1)$ are K dimensional vectors containing the differentially encoded symbols of the K users at the zeroth and previous symbol interval. Each element of $\mathbf{d}(-1)$, $\mathbf{d}(0)$ belongs to an MPSK constellation $F = \{e^{j\frac{2\pi l}{M}}\}_{l=0}^{M-1}$ and the k^{th} element of the vector of the K information symbols $\mathbf{b}(0) \in F^K$ is related to the differentially encoded symbols by $d_k(0) = d_k(-1) b_k(0)$.

The matrix \mathbf{R} is the $KL \times KL$ dimensional signal correlation matrix of the K users' signalling waveforms and their L time translates. The time gap between each translate is the inverse of the signal bandwidth, which is assumed to be equal for all users. Rather than ignoring the inter-symbol interference (ISI) introduced by the multipath channel, we choose to eliminate the ISI by masking out the signal for the relevant times as described in [Var96]. Each user's signalling waveform is normalized to have unit energy so that the diagonal entries of \mathbf{R} are all equal to unity.

The KL dimensional vector of fading channel coefficients $\mathbf{c}(i)$ is defined as $\mathbf{c}^T(i) = [\mathbf{c}_1^T(i), \dots, \mathbf{c}_K^T(i)]$ where $\mathbf{c}_k(i)$

contains the L tap weights of the k^{th} user's L fading paths during the i^{th} symbol interval ($i \in \{-1, 0\}$). Both, $\mathbf{c}(i)$ and the additive noise vectors $\mathbf{n}(i)$, are zero-mean, complex, circularly symmetric Gaussian random vectors. Whereas $\mathbf{n}(-1)$ and $\mathbf{n}(0)$ are statistically independent and have an identical correlation matrix $\frac{1}{2}E[\mathbf{n}(i)\mathbf{n}^\dagger(i)] = \frac{1}{2}\mathbf{R}$ (\dagger denotes the conjugate complex transpose) the vectors of the fading parameters $\mathbf{c}(-1)$ and $\mathbf{c}(0)$ are not statistically independent. Their matrix correlation function $\frac{1}{2}E[\mathbf{c}(i)\mathbf{c}^\dagger(j)]$ is denoted as $\mathbf{\Sigma}(i, j)$; the k^{th} diagonal $L \times L$ submatrix of $\mathbf{\Sigma}(i, j)$, $\mathbf{\Sigma}_{kk}(i, j)$, is the matrix correlation function of the k^{th} user's fading parameters. In stating the MEP rule in Section IV, we will assume that the fading paths of different users are statistically independent of each other, i.e., $\mathbf{\Sigma}(i, j)$ will be block-diagonal with $\mathbf{\Sigma}_{kk}(i, j)$ as diagonal elements. Wide sense stationarity of the fading process allows us to write $\mathbf{\Sigma}(i, i) = \mathbf{\Sigma}(0)$ and $\mathbf{\Sigma}(-1, 0) = \mathbf{\Sigma}^\dagger(0, -1) = \mathbf{\Sigma}(1)$. For our slowly fading channel, where fading coefficients do not change for the duration of two successive symbol intervals, we have $\mathbf{\Sigma}(1) = \mathbf{\Sigma}(0)$. In order to ensure that $\bar{\gamma}r_k$ is the total average signal to noise ratio of user k , the fading coefficients $\mathbf{c}_k(i)$ are normalized such that $\text{Tr}(\mathbf{\Sigma}_{kk}(0)\mathbf{R}_{kk}) = \frac{1}{2}$, where \mathbf{R}_{kk} is the k^{th} $L \times L$ sub-matrix of \mathbf{R} (the k^{th} user's signal correlation matrix).

III. THE GENERALIZED LIKELIHOOD RATIO TEST (GLRT) DETECTOR

As in the single user case presented in [Var97], the problem is to find a good estimate for the data symbols $\mathbf{b}(0)$ based on the observations $\mathbf{q}(-1)$ and $\mathbf{q}(0)$, when only the signal correlation matrix \mathbf{R} is known. To keep the receiver simple, we assume that neither the fading coefficients nor their statistics $\mathbf{\Sigma}(i, j)$ nor the average signal to noise ratios of the users are known. The only information required by the GLRT detector other than the sufficient statistics for the received signal is the correlation matrix \mathbf{R} . The idea of the GLRT detector is to maximize the likelihood of the observations $\mathbf{q}(-1)$ and $\mathbf{q}(0)$ first over the unknown vectors of fading coefficients $\mathbf{c}(-1)$ and $\mathbf{c}(0)$ and then over the differentially encoded data symbols $\mathbf{d}(-1)$ and $\mathbf{d}(0)$. Unfortunately, even in the single user case this rule does not yield meaningful results for $\mathbf{c}(-1) \neq \mathbf{c}(0)$ (cf. [Var97]). To arrive at the decision rule we will assume the slowly fading channel, i.e., $\mathbf{c}(-1) = \mathbf{c}(0) = \mathbf{c}$ so that $\mathbf{\Sigma}(i, j) = \mathbf{\Sigma}(0)$ for the four values of $(i, j) \in \{-1, 0\}^2$.

Conditioned on the fading coefficient vector \mathbf{c} and the differentially encoded symbols ($\mathbf{d}(-1)$, $\mathbf{d}(0)$) the decision statistics $\mathbf{q}(-1)$ and $\mathbf{q}(0)$ are independent Gaussian distributed with correlation matrix \mathbf{R} and mean $\sqrt{\bar{\gamma}} \mathbf{R} \text{diag}\{\mathbf{r}, L\}^{1/2} \text{diag}\{\mathbf{d}(i), L\} \mathbf{c}(i)$ ($i \in \{-1, 0\}$). Considering this distribution, the maximization over \mathbf{c} yields the maximizing vector $\hat{\mathbf{c}}$ as

$$\hat{\mathbf{c}} = \sqrt{\bar{\gamma}}^{-1} [\mathbf{D}^*(-1) \mathbf{R} \mathbf{D}(-1) + \mathbf{D}^*(0) \mathbf{R} \mathbf{D}(0)]^{-1} \times [\mathbf{D}^*(-1) \mathbf{q}(-1) + \mathbf{D}^*(0) \mathbf{q}(0)], \quad (2)$$

where $\mathbf{D}(i) = \text{diag}\{\mathbf{r}, L\}^{1/2} \text{diag}\{\mathbf{d}(i), L\}$. Furthermore, it can be shown that the resulting generalized likelihood function of the pair $\mathbf{q}(-1)$, $\mathbf{q}(0)$ depends only on the M^K possible data

symbols $\mathbf{b}(0)$ rather than on the M^{2K} possible combinations of $\mathbf{d}(-1)$ and $\mathbf{d}(0)$. In what follows, it is convenient to drop the time index in $\mathbf{b}(0)$ and introduce the integer subscript i ($1 \leq i \leq M^K$) indicating the dependence of the transmitted data symbols on the underlying hypothesis H_i . Hence, H_i designates the hypothesis that \mathbf{b}_i is the particular realization of the vector of data symbols $\mathbf{b}(0)$. Furthermore, we define $\mathbf{B}_i = \text{diag}\{\mathbf{b}_i, L\}$ and stack the vectors of observations to define $\mathbf{q}^\top = [\mathbf{q}^\top(-1) \quad \mathbf{q}^\top(0)]$. This notation allows us to write the GLRT decision rule succinctly as

$$\hat{i} = \arg \max_{i \in \{1, 2, \dots, M^K\}} \mathbf{q}^\dagger \mathbf{G}_i \mathbf{q}, \quad (3)$$

$$\mathbf{G}_i = \begin{bmatrix} \mathbf{I} \\ \mathbf{B}_i \end{bmatrix} [\mathcal{R} + \mathbf{B}_i^* \mathcal{R} \mathbf{B}_i]^{-1} \begin{bmatrix} \mathbf{I} & \mathbf{B}_i^* \end{bmatrix}. \quad (4)$$

IV. THE MINIMUM PROBABILITY OF ERROR (MEP) DETECTOR

For the MEP detector, we assume that the statistics of the fading parameters, i.e., the covariance matrices $\Sigma(i, j)$, are known at the receiver. For simplicity, we assume that the fading processes of different users are independent, i.e., the matrices $\Sigma(i, j)$ are block-diagonal. The problem is to maximize the a posteriori probability of the transmitted differential symbols ($\mathbf{d}(-1)$, $\mathbf{d}(0)$) given the decision statistics \mathbf{q} . As each pair ($\mathbf{d}(-1)$, $\mathbf{d}(0)$) is equally probable, because each data vector $\mathbf{b}(0)$ is equally probable, the maximum a posteriori decision rule reduces to the maximum likelihood decision rule. The probability density function (pdf) of \mathbf{q} given ($\mathbf{d}(-1)$, $\mathbf{d}(0)$) is a zero-mean complex Gaussian pdf. Owing to the assumption of independence of fading processes of different users however, this pdf is identical for all pairs ($\mathbf{d}(-1)$, $\mathbf{d}(0)$) that correspond to the same data vector \mathbf{b} . In particular, the covariance matrix of \mathbf{q} under hypothesis H_i is

$$\mathbf{K}_{\mathbf{q}|H_i} = \frac{1}{2} E [\mathbf{q} \mathbf{q}^\dagger] = \begin{bmatrix} \bar{\gamma} \mathcal{R} \Omega \Sigma(-1, -1) \mathcal{R} + \frac{1}{2} \mathcal{R} & \bar{\gamma} \mathcal{R} \Omega \Sigma(-1, 0) \mathbf{B}_i^* \mathcal{R} \\ \bar{\gamma} \mathcal{R} \mathbf{B}_i \Sigma(0, -1) \Omega \mathcal{R} & \bar{\gamma} \mathcal{R} \Omega \Sigma(0, 0) \mathcal{R} + \frac{1}{2} \mathcal{R} \end{bmatrix}, \quad (5)$$

where $\Omega = \text{diag}\{\mathbf{r}, L\}$. Note that we used the fact that the product $\Sigma(i, j) \text{diag}\{\mathbf{d}(i), L\}$ commutes because $\Sigma(i, j)$ is assumed to be block-diagonal with blocks of size $L \times L$ and $\text{diag}\{\mathbf{d}(i), L\}$ is a diagonal matrix with the same element repeated L times on its diagonal. The MEP decision rule can then be stated as

$$\hat{i} = \arg \min_{i \in \{1, 2, \dots, M^K\}} \frac{1}{2} \mathbf{q}^\dagger \mathbf{K}_{\mathbf{q}|H_i}^{-1} \mathbf{q} + \ln(|\mathbf{K}_{\mathbf{q}|H_i}|), \quad (6)$$

where the argument of the minimization is the negative logarithm of the complex gaussian pdf of the decision statistics \mathbf{q} given the data symbols \mathbf{b}_i (corresponding to the hypothesis H_i) were sent. For any matrix \mathbf{M} we define $|\mathbf{M}| = \det(\mathbf{M})$. In contrast to the single-user case, the MEP decision rule for the multiuser CDRF channel is not independent of the determinant of $\mathbf{K}_{\mathbf{q}|H_i}$.

V. ERROR PROBABILITY ANALYSIS

For simplicity, we restrict attention to binary modulation. We give lower and upper bounds on the error probability of the MEP and GLRT detectors described by (6) and (3), respectively. Without loss of generality, we obtain the error probability of the first user.

The upper bound on the error probability of user one is derived by invoking a union bound and the lower bound by only considering the single error events, i.e., events for which there occurs an error for only user one. To derive these bounds we first consider the pair-wise error probability $P_{H_i \rightarrow H_j}$ that a true hypothesis H_i is detected as H_j . This probability can be expressed for both detectors as the probability that a quadratic form in the decision variables \mathbf{q} is smaller than some constant. It will be calculated by invoking the characteristic function of the quadratic form and integrating over the corresponding probability density function (pdf).

Both detectors can be expressed in the form

$$\hat{i} = \arg \min_{i \in \{1, 2, \dots, 2^K\}} \mathbf{q}^\dagger \mathbf{F}_i \mathbf{q} + c_i. \quad (7)$$

For the MEP detector $\mathbf{F}_i = \frac{1}{2} \mathbf{K}_{\mathbf{q}|H_i}^{-1}$ and $c_i = \ln(|\mathbf{K}_{\mathbf{q}|H_i}|)$. For the GLRT detector $\mathbf{F}_i = -\mathbf{G}_i$ and $c_i = 0$. In the remainder of this section we express everything in terms of \mathbf{F}_i , c_i , and the covariance matrix $\mathbf{K}_{\mathbf{q}|H_i}$ of the decision statistics \mathbf{q} . The probability $P_{H_i \rightarrow H_j}$ is the probability that the decision statistic $\mathbf{q}^\dagger \mathbf{F}_j \mathbf{q} + c_j$ is smaller than $\mathbf{q}^\dagger \mathbf{F}_i \mathbf{q} + c_i$

$$\begin{aligned} P_{H_i \rightarrow H_j} &= P(\mathbf{q}^\dagger \mathbf{F}_j \mathbf{q} + c_j < \mathbf{q}^\dagger \mathbf{F}_i \mathbf{q} + c_i) \\ &= P(\mathbf{q}^\dagger \mathbf{F}_{ij} \mathbf{q} < c_{ij}), \end{aligned} \quad (8)$$

where $\mathbf{F}_{ij} = \mathbf{F}_j - \mathbf{F}_i$ and $c_{ij} = c_i - c_j$. As \mathbf{F}_{ij} is Hermitian for both decision rules and \mathbf{q} is a zero-mean, complex Gaussian random vector, the characteristic function of the quadratic form $\mathbf{q}^\dagger \mathbf{F}_{ij} \mathbf{q}$ can be found as in Appendix B of [SBS96] as

$$E[e^{-s \mathbf{q}^\dagger \mathbf{F}_{ij} \mathbf{q}}] = \frac{1}{\prod_{l=1}^{l=N} \lambda_l \left(s + \frac{1}{\lambda_l}\right)}, \quad (10)$$

where N is the number of non-zero eigenvalues λ_l of $2 \mathbf{K}_{\mathbf{q}|H_i} \mathbf{F}_{ij}$.¹ With the help of this, the probability $P_{H_i \rightarrow H_j}$ may be expressed in the form

$$P_{H_i \rightarrow H_j} = \int_{-\infty}^{c_{ij}} \frac{1}{2\pi j} \int_{-j\infty+\epsilon}^{j\infty+\epsilon} \frac{e^{sf}}{\prod_{l=1}^{l=N} \lambda_l \left(s + \frac{1}{\lambda_l}\right)} ds df. \quad (11)$$

Interchanging the order of integration and evaluating the inverse Laplace transform using complex contour integrals allows us to write

$$\begin{aligned} P_{H_i \rightarrow H_j} &= \\ &= - \sum_{m=1}^{m=M} \text{Res} \left(\frac{e^{s c_{ij}}}{s \prod_{l=1}^{l=N} \lambda_l \left(s + \frac{1}{\lambda_l}\right)}, s_m = -\frac{1}{\lambda_l} > 0 \right) \end{aligned} \quad (12)$$

¹The differences in our notation and the one used in [SBS96] arise, because we define the correlation matrix as the complex conjugate of the definition used in [SBS96]. Furthermore, we incorporate the factor of 2 in the definition of the eigenvalues rather than in the characteristic function and use the two-sided Laplace transform instead of the Fourier transform.

for $c_{ij} \leq 0$ and M being the number of negative eigenvalues of $2 \mathbf{K}_{\mathbf{q}|H_i} \mathbf{F}_{ij}$. For $c_{ij} > 0$ the probability is calculated as

$$P_{H_i \rightarrow H_j} = \sum_{m=1}^{m=M} \text{Res} \left(\frac{1}{s \prod_{l=1}^{l=N} \lambda_l \left(s + \frac{1}{\lambda_l} \right)}, s_m = -\frac{1}{\lambda_l} > 0 \right) + \sum_{n=1}^{n=N-M} \text{Res} \left(\frac{e^{s c_{ij}} - 1}{s \prod_{l=1}^{l=N} \lambda_l \left(s + \frac{1}{\lambda_l} \right)}, s_n = -\frac{1}{\lambda_l} \leq 0 \right). \quad (13)$$

In both equations the residue of a function $f(s)$ in a pole a of multiplicity m is defined to be

$$\text{Res}(f(s), a) = \frac{1}{(m-1)!} \lim_{s \rightarrow a} \frac{d^{m-1}}{ds^{m-1}} [(s-a)^m f(s)]. \quad (14)$$

This notation is especially convenient for poles of multiplicity greater than one.

Having obtained the probability $P_{H_i \rightarrow H_j}$ we union bound $P_{e|H_i}$, the error probability of user one conditioned on hypothesis H_i . Computing $P_{e|H_i}$ precisely would require the evaluation of the probability of the union of all 2^{K-1} possible error events where an error for user one occurs. This probability is upper bounded by the sum of the probabilities of those error events so that

$$P_{e|H_i} \leq \sum_{\substack{\forall j \in \{1, \dots, 2^K\} \text{ s.t.} \\ [\mathbf{b}_j]_1 \neq [\mathbf{b}_i]_1}} P_{H_i \rightarrow H_j}, \quad (15)$$

where $[\mathbf{b}_i]_k$ denotes the k^{th} element of the vector of data symbols corresponding to hypotheses H_i . $[\mathbf{b}_j]_1 \neq [\mathbf{b}_i]_1$ indicates the error in the detection of the first user's data symbol. Averaging over all 2^K equally probable hypotheses H_i yields the upper bound on the first user's error probability P_e

$$P_e = \frac{1}{2^K} \sum_{i=1}^{2^K} P_{e|H_i} \leq \frac{1}{2^K} \sum_{i=1}^{2^K} \sum_{\substack{\forall j \in \{1, \dots, 2^K\} \text{ s.t.} \\ [\mathbf{b}_j]_1 \neq [\mathbf{b}_i]_1}} P_{H_i \rightarrow H_j}. \quad (16)$$

A lower bound on the first user's error probability is simply obtained by averaging over all 2^K single error events where an error only occurs for the first user so that

$$P_e \geq \frac{1}{2^K} \sum_{\substack{\forall j \in \{1, \dots, 2^K\} \text{ s.t. } [\mathbf{b}_j]_1 \neq [\mathbf{b}_i]_1 \\ [\mathbf{b}_j]_k = [\mathbf{b}_i]_k, 2 \leq k \leq K}} P_{H_i \rightarrow H_j}. \quad (17)$$

With this, and equations (12),(13), and (16) the bounds on error probability are fully specified.

VI. NUMERICAL RESULTS

In this section we present numerical examples. Six users are considered who employ length-31 Gold-sequences as in [Var97]. The signal correlation matrix \mathcal{R} is calculated as defined in [Var96] using the ISI-IUI mask described therein. For the decorrelating detectors the correlation matrix is the inverse of the upper left $L \times L$ submatrix of the inverse of the multiuser correlation matrix \mathcal{R} . There are four paths for each user, which fade independently. The average relative power of each fading path is chosen according to the simplified GSM 'urban' test profile. Normalizing $\Sigma(0)$ properly leads to $\Sigma_{kk}(0) = \text{diag}\{0.11, 0.21, 0.13, 0.05\}$ for all users. The error probabilities displayed in the figures are not calculated using the residue method used in the analysis of the previous section, because such a computation is numerically unstable. Instead, the inverse Laplace transform of (11) (after the interchange of integration) is computed numerically using a saddlepoint technique. A description of this numerically stable integration method can be found for example in [Hel95].

Figure 1 compares all of the presented detectors for slow fading and equal energies of all users ($E_k/E_1 = 1$). Applying the single-user MEP detector to the decorrelated multiuser channel as proposed in [Var97] gives an improvement of 5dB over the ad-hoc decorrelating equal gain combining (D-EGC) detector of [ZB96], [Zvo94], and [HS94]. However, as we pointed out earlier, the multiuser MEP can improve significantly on the decorrelating approaches: in this example it outperforms the decorrelating single-user MEP (D-SU-MEP) detector by 6dB, and hence the D-EGC detector by 11dB. As in the single-user channel, the MEP and GLRT detectors' performances are close. The multiuser GLRT detector lies, as one might expect, in between the multiuser MEP and D-SU-MEP detector. Note that the bounds we obtained on the BER of the detectors converge, thereby justifying our choice of the single error events for the lower bound. In contrast to coherent detection, where the asymptotic efficiency is one (cf. [Var96]), one cannot expect the same for DPSK modulation, as can be seen from the 2dB gap between the single-user and multiuser channel for MEP detection. This also implies that the 3dB gap between the MEP detectors for noncoherent DPSK and coherent BPSK in a single-user CDRF channel proved in [Var98] will not generalize to the multiuser channel. Since the asymptotic efficiency of coherent MEP detection is unity, this gap can be observed in Figure 1.

Figure 2 shows the same detectors as Figure 1 but here the energy of the user of interest (user 1) is ten times higher than the energy of the interfering users. The bounds on the error probability of the GLRT and MEP detectors still converge but are looser. Note that for low SNRs the lower bound of the MEP is closer to the single user MEP than for equal energies. This hints that the multiuser MEP detector collapses to the single user MEP detector when the energy of the interfering users tends to zero, which can indeed be shown analytically. Hence, one might argue that the lower bound captures the true BER on the MEP and the upper bound is loose, because multiple error events in the union bound become more likely for weak interfering users. For strong interfering users (not shown in a plot) the upper bounds on the MEP and GLRT detectors be-

come tighter, as the multiple error events in the union bound become less likely. Interestingly, the gaps to the single-user MEP and between the MEP and GLRT are asymptotically the same, independent of the energy of the interfering users (as long as those are not zero). The decorrelating approaches are naturally not affected by either an increase or decrease in the energy of the interfering users.

Figure 3 depicts the BER of the MEP and D-EGC detectors for fast fading with fade rate $\rho = 0.975$ and equal energies for all users. For simplicity, the fading correlation matrices are chosen as $\Sigma(1) = \rho\Sigma(0)$. This choice implies that the relative movement between the users and a base station is the same for all users, which is clearly unlikely in practical applications. However, the basic system behavior is captured by this choice. The fade rate ρ is connected to the normalized Doppler bandwidth $B_D T$ by $\rho = J_0(\pi B_D T)$ for fading with power spectrum density given by Jakes' model [Jak93]. The bounds on the BER of the MEP detector still converge. For a medium SNR of 15dB the D-EGC has a dismal BER of 0.2 making it essentially useless for this practically important SNR. The BER for the D-SU-MEP can improve on this BER by a factor of ten and the multiuser MEP by a factor of 100, making applications possible.

In Figure 4 the curves of Figure 3 are continued for high values of SNR. It also includes the performances of the detectors for a fade rate ρ of 0.9. Note now the flooring of the BERs. Moreover, not surprisingly, all detectors perform worse for the faster fading case and the BER floor is considerably higher. The multiuser MEP and D-SU-MEP reach the same error floor as the MEP in the single-user channel for both fade rates. This shows that for very high SNRs, fast fading is the limiting factor on system behavior. Whereas the BER floor reached by the D-EGC might be regarded as acceptable in comparison to the D-SU-MEP or the MEP, for practically relevant ranges of the SNR the performance of the D-EGC is not acceptable, as was pointed out in the discussion of Figure 3.

Figure 5 shows that for fast fading, the lower bound on the multiuser MEP detector also approaches the single-user MEP detector performance (as in slow fading) when the energy of the interfering users is low ($E_k/E_1 = 0.01$ for $k > 1$). This implies also that the error floor of the multiuser MEP detector does not change and seems to be independent of the interfering users' energies. The upper bound on the BER of the MEP detector is very loose as multiple error events are very likely and hence contribute substantially in the union bound. Nevertheless, the bounds converge for high SNR and one might argue as with Figure 2 that the lower bound captures the true BER. As in slow fading, the BERs of the decorrelating detectors are independent of the interfering users' energy.

Figure 6 strengthens our claim that the BER floor of the MEP is independent of the interfering users' energies. In this figure, they are 100 times higher than the first user's energy. As obviously multiple error events in the MEP rule are very unlikely for strong interfering users, the upper bound on the BER of the MEP detector coincides with the lower bound which makes it invisible in the figure. For low to medium SNRs the performance of the MEP deteriorates when compared to the case where all users have the same energy (Figure 4).

VII. CONCLUSIONS

With the exception of [Var97], previous approaches to DPSK detection in diversity Rayleigh fading channels have so far been guided by the ad-hoc post-decorrelative equal-gain combining rule. [Var97] introduced the optimum detection approach for the single-user DPSK CDRF channel. This work systematically extends the single-user approach to the multi-user channel. The performance of the MEP multiuser detector shows that better than post-decorrelative detectors are necessary; applying the optimum single-user detector to the decorrelated multi-user observations results in a loss of as much as 6dB in our example.

In contrast to the single-user case, the multiuser GLRT detector cannot compete quite as well with the MEP detector for slow fading; that its performance degrades for fast fading further (not shown in a figure) is not surprising; it is derived under the assumption of constant fading coefficients over two successive symbol intervals. Its simplicity (no knowledge of the fading parameters, their statistics, or the users' energies is required) may be in favor of its implementation for slowly fading channels. A factor that precludes the widespread use of the detectors presented here is their exponential complexity in the number of users. Detectors which are far less complex but still retain near-optimum performance, where the ultimate benchmark is the multiuser MEP detector, have yet to be found.

REFERENCES

- [Hel95] Carl W Helstrom. *Elements of Signal Detection & Estimation*. Prentice-Hall, Englewood Cliffs, NJ, 1995.
- [HS94] H C Huang and S C Schwartz. A comparative analysis of linear multiuser detectors for fading multipath channels. In *Proc. IEEE GLOBECOM*, pages 11–15, December 1994.
- [Jak93] W C Jakes. *Microwave Mobile Communications*. An IEEE Press Classic Reissue, New York, 1993. Originally An American Telephone and Telegraph Company Publication, 1974.
- [SBS96] M Schwartz, W R Bennett, and S Stein. *Communication Systems and Techniques*. An IEEE Press Classic Reissue, New York, 1996. Originally A McGraw-Hill Publication, 1966.
- [Var96] M K Varanasi. Parallel group detection for synchronous CDMA communication over frequency-selective Rayleigh fading channels. *IEEE Trans. Inform. Theory*, 43(1):116–128, January 1996.
- [Var97] M K Varanasi. A systematic approach to noncoherent detection for DPSK modulation in single-user correlated diversity Rayleigh fading channels with applications to post-combining detection. In *Proc. Conf. Info. Science and Syst.*, 1997.
- [Var98] M K Varanasi. Optimum DPSK receivers for the correlated diversity Rayleigh fading channel. *To appear in IEEE Trans. Commun.*, 1998.
- [WDH94] H-Y Wu and A Duel-Hallen. Channel estimation and multiuser detection for frequency-nonselective fading synchronous CDMA channels. In *Proc. 32nd Annual Allerton Conf. on Communication, Control, and Computing*, pages 335–344, 1994.
- [ZB96] Z Zvonar and D Brady. Linear multipath-decorrelating receivers for CDMA frequency-selective fading channels. *IEEE Trans. Commun.*, 44(6):650–653, June 1996.
- [Zvo94] Z Zvonar. Multiuser detection and diversity combining for wireless CDMA systems. In Jack M Holtzmann and D J Goodman, editors, *Wireless and Mobile Communications*. Kluwer Academic Press, 1994.

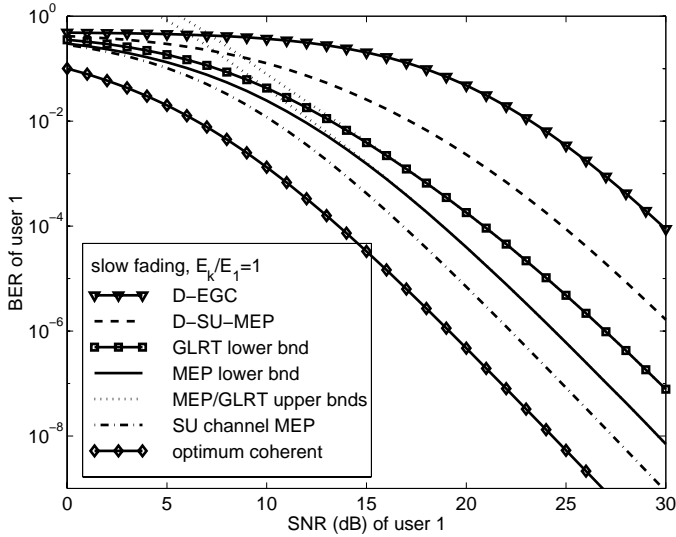


Fig. 1. BER comparison of the decorrelating equal-gain combiner, post-decorrelative single-user MEP, multiuser GLRT and MEP, single-user channel MEP, and optimum multiuser coherent detectors. There is a 11dB gap between the D-EGC and the multiuser MEP detector.

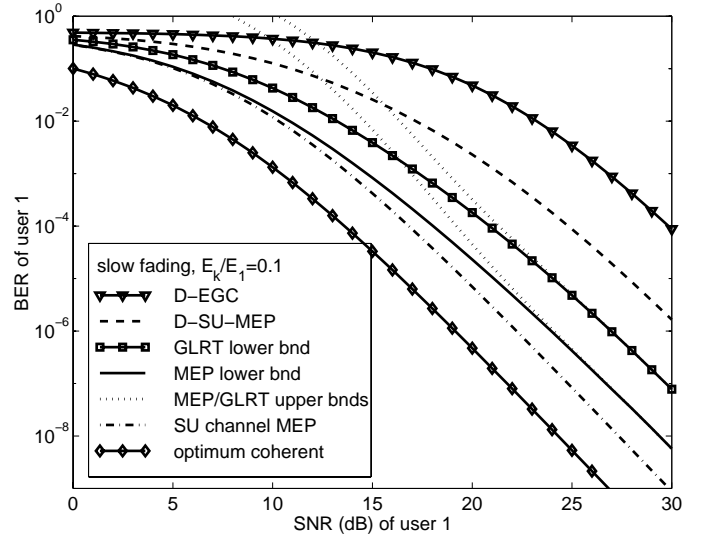


Fig. 2. When the power of the interfering users decreases, the upper bounds on the MEP and GLRT detectors become looser, but converge asymptotically (as they do in Figures 1–6).

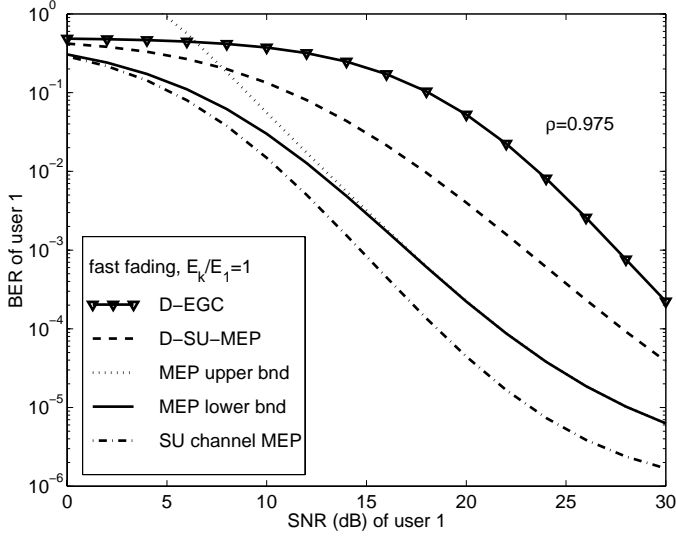


Fig. 3. BER comparison of the D-EGC, D-SU-MEP, multiuser MEP, and SU channel MEP detectors for fast fading and medium SNRs. All users have the same power. At 15dB, the BER of the multiuser MEP is about 100 times smaller than the BER of the D-EGC.

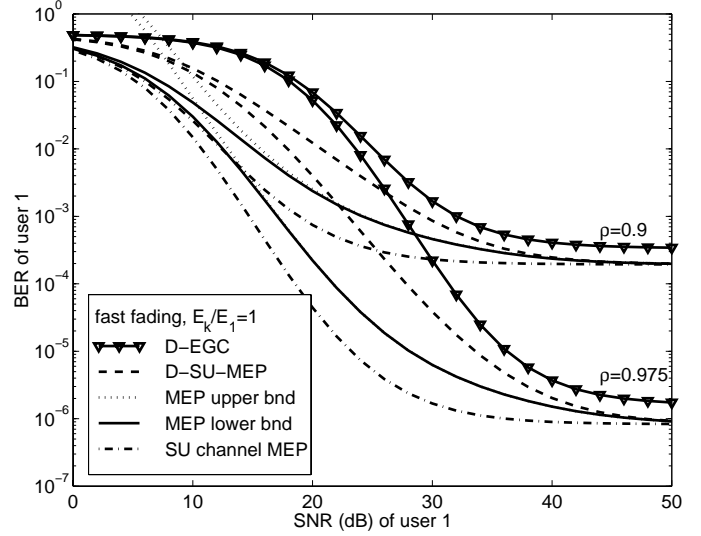


Fig. 4. The same settings as in Figure 3 to the left, but plotted for high SNRs, when the error floor is reached. For faster fading, the performance of all detectors degrades, as expected.

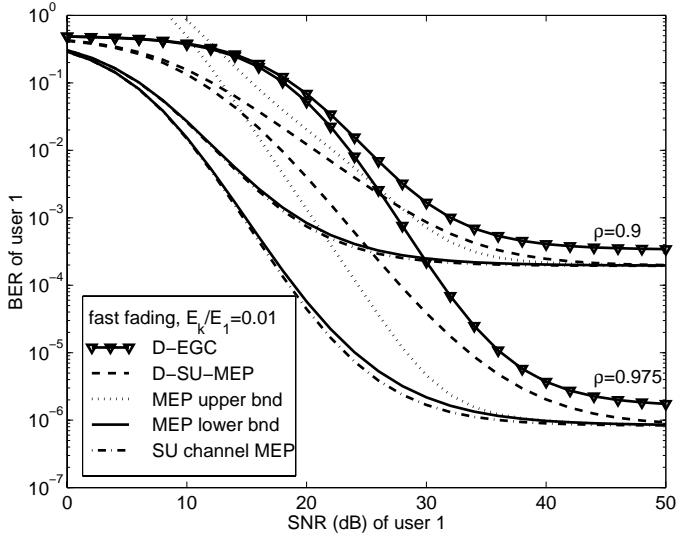


Fig. 5. When the power of the interfering users becomes very weak, the upper bound on the MEP is looser. The true BER may be closer to the lower bound as described in Section VI.

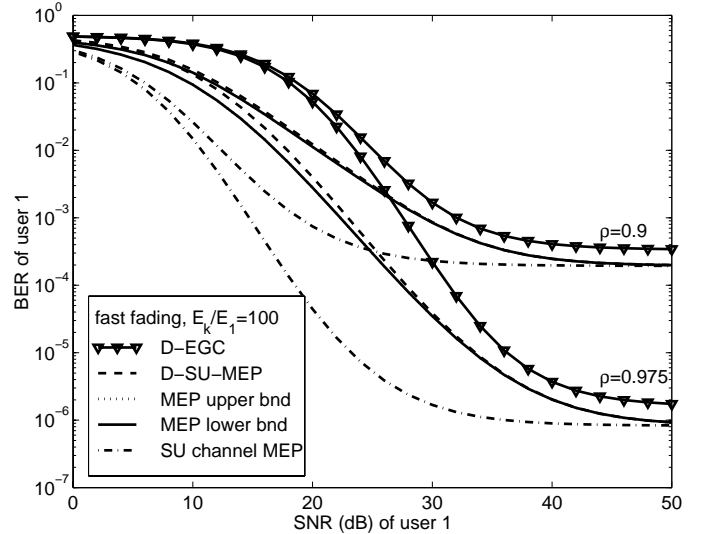


Fig. 6. When the power of the interfering users increases, the upper bound on the BER of the MEP becomes tighter and the BER of the MEP increases.